

AD-A169 100

DOUBLE-TAILED SURFACTANTS: THE EFFECT OF HYDROCARBON
CHAIN STRUCTURE ON P. (U) TENNESSEE UNIV KNOXVILLE DEPT
OF CHEMISTRY L J MAGID 13 MAY 86 ARO-18631. 5L-CH

1/1

UNCLASSIFIED

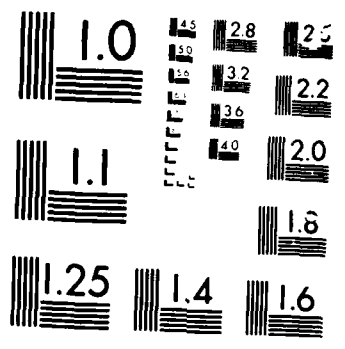
DAAG29-82-K-0115

F/G 7/4

ML



END



MICROCOPY

1011

AD-A169 100

ARO 18631.5-CH

②

DOUBLE-TAILED SURFACTANTS: THE EFFECT OF HYDROCARBON
CHAIN STRUCTURE ON PHASE BEHAVIOR

FINAL REPORT

Author: Linda J. Magid

13 May 1986

U. S. Army Research Office

Grant # DAAG 29-82-K-0115

The University of Tennessee

DTIC FILE COPY

DTIC
SELECTED
JUN 25 1986
S E D

[Faint, illegible stamp]

AD-A169100

UNCLASSIFIED

SECURITY CLASSIFICATION OF THIS PAGE (When Data Entered)

REPORT DOCUMENTATION PAGE		READ INSTRUCTIONS BEFORE COMPLETING FORM
1. REPORT NUMBER ARO 18631.5-CH	2. GOVT ACCESSION NO. N/A	3. RECIPIENT'S CATALOG NUMBER N/A
4. TITLE (and Subtitle) DOUBLE-TAILED SURFACTANTS: THE EFFECT OF HYDROCARBON CHAIN STRUCTURE ON PHASE BEHAVIOR	5. TYPE OF REPORT & PERIOD COVERED Final: 4/26/82-2/28/86	
	6. PERFORMING ORG. REPORT NUMBER	
7. AUTHOR(s) Linda J. Magid	8. CONTRACT OR GRANT NUMBER(s) DAAG 29-82-K-0115	
9. PERFORMING ORGANIZATION NAME AND ADDRESS Department of Chemistry University of Tennessee Knoxville, TN 37996-1600	10. PROGRAM ELEMENT, PROJECT, TASK AREA & WORK UNIT NUMBERS	
11. CONTROLLING OFFICE NAME AND ADDRESS U. S. Army Research Office Post Office Box 12211 Research Triangle Park, NC 27709	12. REPORT DATE 5/13/86	
	13. NUMBER OF PAGES 16	
14. MONITORING AGENCY NAME & ADDRESS (if different from Controlling Office)	15. SECURITY CLASS. (of this report) Unclassified	
	15a. DECLASSIFICATION/DOWNGRADING SCHEDULE	
16. DISTRIBUTION STATEMENT (of this Report) Approved for public release; distribution unlimited.		
17. DISTRIBUTION STATEMENT (of the abstract entered in Block 20, if different from Report) NA		
18. SUPPLEMENTARY NOTES The view, opinions, and/or findings contained in this report are those of the author(s) and should not be construed as an official Department of the Army position, policy, or decision, unless so designated by other documentation.		
19. KEY WORDS (Continue on reverse side if necessary and identify by block number) Micelles, Microemulsions, double-tailed surfactants, scattering, conductimetry, NMR, EMF		
20. ABSTRACT (Continue on reverse side if necessary and identify by block number) Micelles of several double-tailed surfactants, some water-soluble, others oil-soluble, have been synthesized and their micellar solutions studied by several experimental techniques: small-angle scattering conductimetry, ²³ Na NMR, ion-selective electrodes. Their micellar properties have been compared and contrasted to those of single-tailed surfactants.		

TABLE OF CONTENTS

	<u>Page</u>
Statement of the Problem Studied	1
Summary of the Results Obtained	1
Publications	4
Participating Scientific Personnel	4
Table I	5
Table II	5
Figure 1	6
Figure 2	7
Figure 3	7
Figure 4	8
Figure 5	8
Figure 6	9
Figure 7	10
Figure 8	10
Figure 9	11
Figure 10	11
Figure 11	12
Figure 12	13
Figure 13	13

Accepted For	
NTIS GFA&I	<input checked="" type="checkbox"/>
ERIC JAF	<input type="checkbox"/>
Unannounced	<input type="checkbox"/>
Justification	
By _____	
Distribution/	
Availability Codes	
Available for	
Dist	Special
A-1	



LIST OF TABLES AND FIGURES

- TABLE I: c.m.c.'s, c_t 's and Dissociation Degrees for Micelles of 5 and 6.
- TABLE II: Aggregation Behavior of Oil-Soluble Surfactants.
- Figure 1: Surfactants whose normal micelles were studied.
- Figure 2: Specific conductivity vs. concentration for 5 in H₂O at 45°C.
- Figure 3: EMF measurements for 2 in H₂O at 45°C.
- Figure 4: EMF measurements for 1 in H₂O at 45°C.
- Figure 5: Electrode construction for sensing anionic surfactants.
- Figure 6: Micellar aggregation number vs. concentration of micellized surfactant: 3 (o); 8 (■); 2 (*); 1 (●).
- Figure 7: Fit of experimental SANS data as a function of added NaCl for 7 (a) and 8 (b). Full lines: Calculated intensities; dotted line, $S(Q)$; dashed line, $P(Q)$.
- Figure 8: Plot of the aggregation numbers and extent of counterion dissociation for 7 (o) and 8 (□).
- Figure 9: Fit of the scattering curve for 0.041 M 5, assuming the micelles to be prolate ellipsoids.
- Figure 10: Micellar aggregation numbers for CTAB and 5; axial ratios for 5.
- Figure 11: 2-D contour plots of scattered intensities for shear-aligned micellar solutions. G is the shear rate.
- Figure 12: Synthetic scheme for oil-soluble surfactants.
- FIGURE 13: Oil-soluble surfactants.

Statement of the Problem Studied

The formation by double-tailed ionic surfactants of normal micelles in water, reverse micelles in a hydrocarbon solvent and microemulsions in surfactant/hydrocarbon/water systems was proposed to possess quantitative and qualitative differences from aggregation by the analogous single-tailed surfactants. In comparing the two classes, with respect to normal micelles the following questions were of interest: (1) how does micelle size change? (2) how does the extent of counterion binding change? (3) what transitions in micelle shape occur as surfactant concentration is increased? (4) how does the propensity for micellar growth with increasing surfactant concentration depend upon surfactant structure? The experimental techniques employed included conductimetry, EMF measurements (both surfactant-selective and counterion-selective electrodes were used), ^{23}Na NMR, ^1H NMR and small-angle scattering (both light and neutron).

Sodium 23 Hydroxide
Summary of the Results Obtained

A. Normal Micelles in Water (Refs. 1-6).

The surfactants studied are given in Figure 1. All of these materials, except for CTAB, were prepared in our laboratories. Critical micelle concentrations were usually determined using conductimetry or EMF measurements (counterion-selective electrodes); for compounds 5 and 6 a second cmc (c_t) was found, which is characteristic of a change in micellar shape and a marked propensity for growth (with associated decrease in fraction of dissociated counterions, α). Figure 2 presents conductivity data for compound 5; Table I summarizes data on counterion binding for compounds 5 and 6. Figure 3 presents representative EMF data for 2. We also made an extensive study of the construction of surfactant-selective electrodes for our systems; Figure 4 presents EMF data for 1. Figure 5 shows a schematic of the electrode system. The Nernstian response of both the counterion-selective and surfactant ion-selective electrodes below the cmc indicate that little if any pre-micellar association is occurring.

Static small-angle neutron scattering (SANS) data have been acquired for all eight surfactants; for some of them, the effect of

*References are coded to the list of publications.

added supporting electrolyte on micellar growth has been studied. In addition, for 1, 2, 7 and 8 external contrast variation has been used in order to estimate the size of the water-excluded hydrocarbon micellar cores. Very recently we have been working on the synthesis of 2 with perdeuterated n-heptyl tails. SANS measurements on micelles formed from mixtures of the deuterated and protiated forms of the surfactant will allow an even better assessment of the dry hydrocarbon core's size for 2.

Figure 6 summarizes micellar aggregation numbers as a function of stoichiometric surfactant concentration at 45°C in D₂O for 1, 2, 3 and 8. We have found that the propensity for micelle growth increases as the micellar solubility limit decreases. We define the micellar solubility limit as the surfactant concentration in the binary surfactant-water phase diagram where the isotropic micellar solution first coexists with a second (liquid crystalline) phase. For all of these double-tailed surfactants, the first liquid crystalline phase encountered is lamellar; close to the solubility limit the micelles are disclike in shape (oblate ellipsoidal). However, some of them give scattering patterns characteristic of prolate ellipsoidal particles at intermediate concentrations.

Figure 7 presents fits for SANS data on 0.07 M solutions of 7 and 8 at 65°C, containing various amounts of NaCl. Figure 8 summarizes the micellar aggregation numbers and counterion binding (expressed as Z/\bar{n} , which is equal to $1-\alpha$) extracted from the fits. Note that the double-tailed surfactant shows substantially less counterion binding and has micelles which grow more rapidly with increases in surfactant concentration.

Micelles of 5 and 6 in D₂O at 45°C have been studied by SANS; the fit, assuming the micelles are prolate ellipsoids, is shown in Figure 9 for 0.041 M 5. Figure 10 compares aggregation numbers for 5 and 4; note that there is (apparently) a decline in micelle size for 5 at higher concentrations. This decline begins when the average center-to-center separation of the micelles is less than twice the ellipsoid's semimajor axis. Addition of NaCl to solutions of 5 induces enormous micellar growth. Figure 11 shows the anisotropic scattering patterns produced

when these elongated micelles are aligned in a shear flow. These patterns are the signature for rodlike micelles.

B. Reverse Micelles in Isooctane (Ref. 5).

Three potentially oil-soluble surfactants were prepared, using the scheme of Figure 12: BC8ASP, NC8ASP and the amide analogue of BC8ASP, (designated BC8AMP). All three surfactants were hygroscopic; the impure materials were yellow oils which are purified by lyophilization and/or recrystallization. None of the three is soluble in water at 25 or 45°C at their (estimated) cmc's, unlike their sulfosuccinate analogue Aerosol OT (same hydrophobe structure as BC8ASP, (see Figure 13.), which does have a small normal micellar region. We also sonicated aqueous dispersions of the three surfactants, but they did not form vesicles. BC8ASP was not soluble in aliphatic hydrocarbon solvents either, but B and NC8ASP were. However, unlike AOT, in isooctane (2,2,4-trimethylpentane) they solubilized relatively little water (water-to-surfactant molar ratio less than three).

We determined apparent micellar sizes in deuterated isooctane for the aspartate surfactants using SANS; AOT reverse micelles were studied also in d-IOT to provide a direct comparison. Since the continuous phase (the isooctane) penetrates a few Å into the surfactant layer, the radii obtained were a bit less than the actual micellar dimensions. Thus for AOT, which forms minimum sphere micelles of 15 Å (evaluated by light scattering) in isooctane, we found an R_{app} of 13-14 Å. As expected, the aspartate micelles having the longer hydrocarbon tails have the largest R_{app} observed. Table II summarizes the aggregation behavior.

C. Three Component Microemulsions Containing Double-Tailed Anionic Surfactants.

We attempted to produce microemulsions analogous to those of Evans and coworkers, who have used the cationic double-tailed surfactant, dimethyldidodecylammonium bromide (DDAB). With water and a variety of n-alkanes, sodium bis(n-nonyl) and (n-decyl)sulfosuccinates failed to produce one phase regimes at any composition. We were able to form microemulsions using a mixed surfactant of Aerosol OT plus sodium dodecylsulfate, but these lie near the oil corner of the phase diagram and are therefore probably conventional water-in-oil micromulsions.

Publications

1. Magid, L. J.; Butler, P. D.; Daus, K. A. "Aggregation of Double-Tailed Surfactants in Water," Proceedings of the 1983 CSL Conference on Chemical Defense Research.
2. Magid, L. J.; Daus, K.; Butler, P.; Quincy, R. "Aggregation of Sulfosuccinate Surfactants in Water," J. Phys. Chem. 1983, 87, 5472-5478.
3. Triolo, R.; Hayter, J. B.; Magid, L. J.; Johnson, J. S. "Small-Angle Neutron Scattering from H₂O/D₂O Solutions of a Sodium Alkylbenzenesulfonate Having a Branched Alkyl Group," J. Chem. Phys. 1983, 79, 1977-1980.
4. Magid, L. J.; Martin, C. A.; Caponetti, E. "Small-Angle Neutron Scattering (SANS) Studies of Single- and Double-Tailed Surfactants in Water," Proceedings of the 1984 Chemical Research and Development Center Conference on Chemical Defense Research.
5. Magid, L. J. "The Elucidation of Micellar and Microemulsion Architecture using Small-Angle Neutron Scattering," Colloids and Surfaces, in press.
6. Caponetti, E.; Triolo, R.; Ho, P. C.; Johnson, J. S.; Magid, L. J.; Butler, P.; Daus, K. "A Small-Angle Neutron Scattering (SANS) Study of Micellar Structure and Growth of a Straight-Chain Benzene Sulfonate. Comparison with an Isomeric Branched-Chain Surfactant," J. Colloid Interface Sci., in pres.

Participating Scientific Personnel

1. Postdoctoral Associate
Dr. Craig Martin - 11/1/83 - 9/30/84
2. Graduate Students
Paul Butler - GTA/GRA - 9/1/82 - present
Kimberlee Daus Payne - GTA/GRA - 9/1/82 - present
Michael Carver - GTA - 9/1/83 - 3/31/84
Joel Phelps - GTA - 9/1/83 - 8/15/85
3. Summer Research Students
Roger Quincy - 6/1/83 - 7/31/83
Stuart Berr - 6/1/83 - 8/31/83

TABLE I: c.m.c.'s, c_t 's and Dissociation Degrees for Micelles of 5 and 6.

from conductimetry:	c.m.c., mM	c_t , mM	α_I	α_{II}
<u>6</u>	2.6	21.8	0.53	0.34
<u>5</u>	0.29	1.5	0.73	0.44

from EMF measurements:	[<u>6</u>], mM	α	[<u>5</u>], mM	α
	1.33	0.51	0.45	0.60
	1.62	0.45	0.86	0.59
	1.96	0.43	1.29	0.56
	2.82	0.42	2.32	0.46

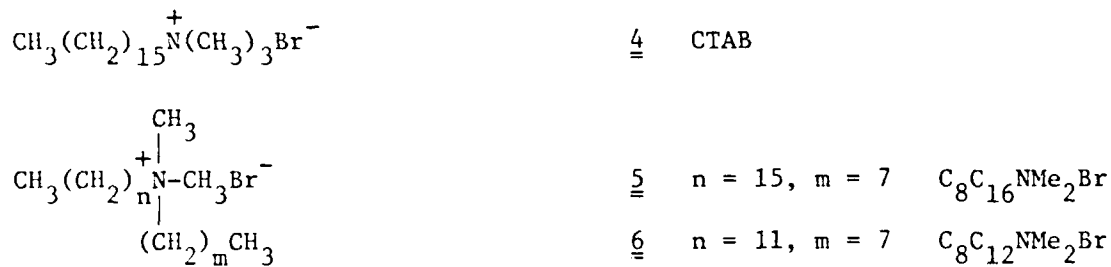
TABLE II: Aggregation Behavior of Oil-Soluble Surfactants.

Surfactant	$R_{app}, \overset{\circ}{A}$	\bar{n}
0.10 M AOT	13.8	19
0.20 M AOT	13.0	16
0.10 M NC8ASP	14.3	23
0.20 M BC8ASP	12.0	13
0.30 M BC8ASP	11.2	11
0.40 M BC8ASP	10.4	9

Sulfosuccinates:



Tetraalkylammonium bromides:



Alkylbenzenesulfonates:

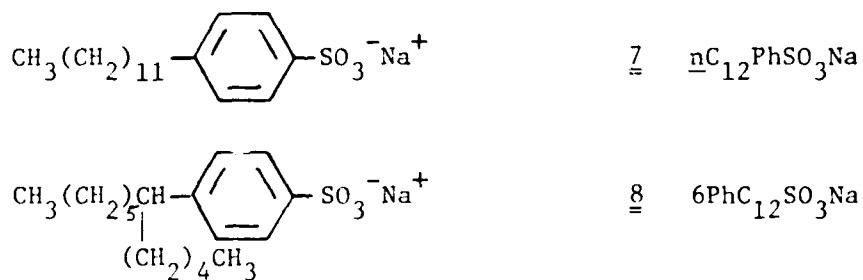


Figure 1. Surfactants whose normal micelles were studied.

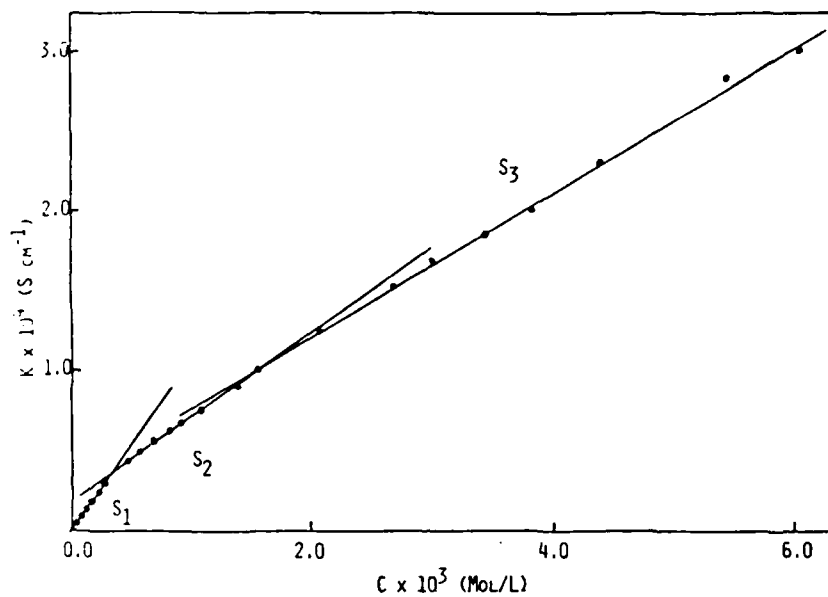


Figure 2. Specific conductivity vs. concentration for 5 in H_2O at 45°C .

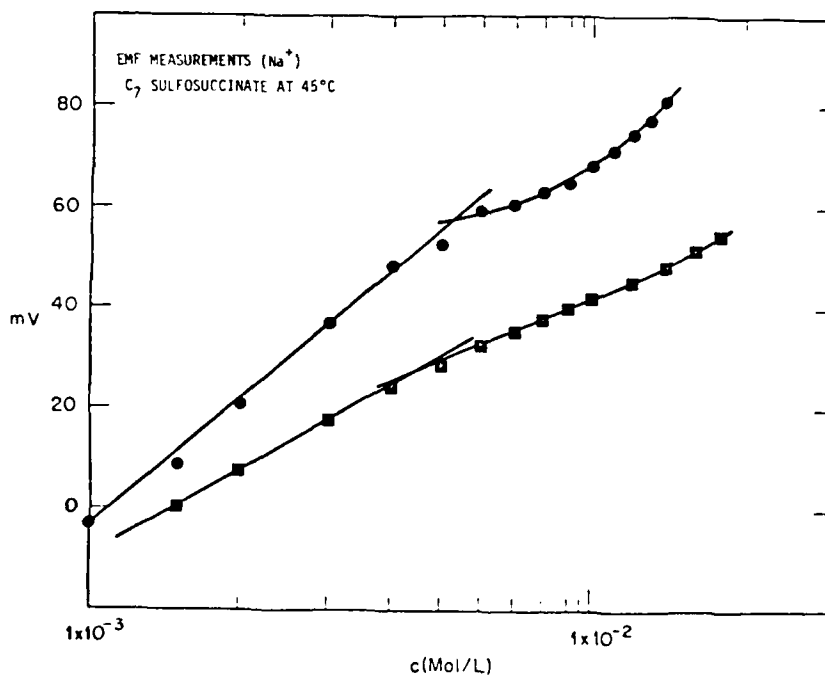


Figure 3. EMF measurements for 2 in H_2O at 45°C .

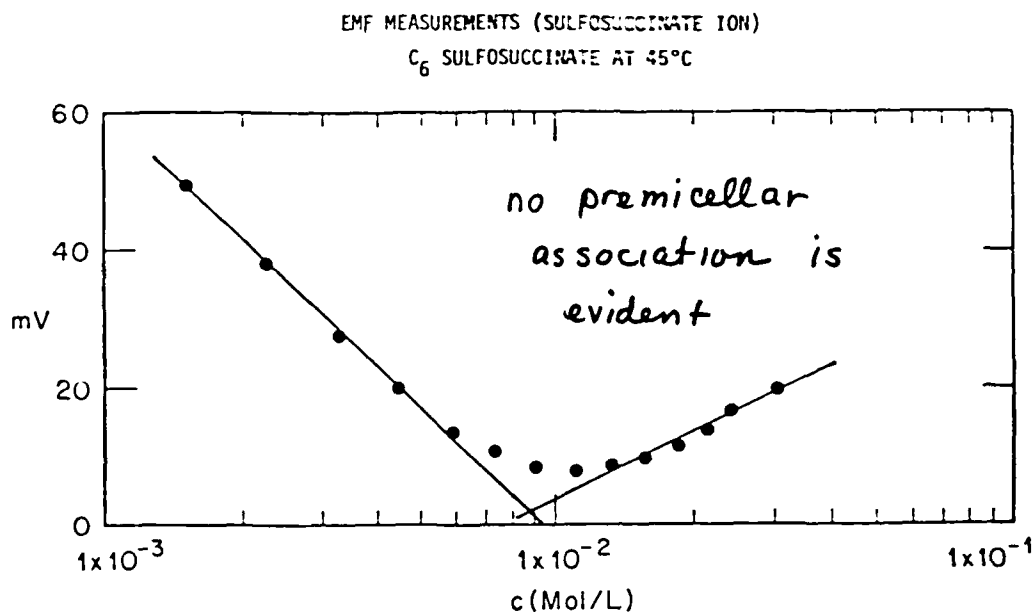


Figure 4. EMF measurements for $\underline{1}$ in H₂O at 45°C.

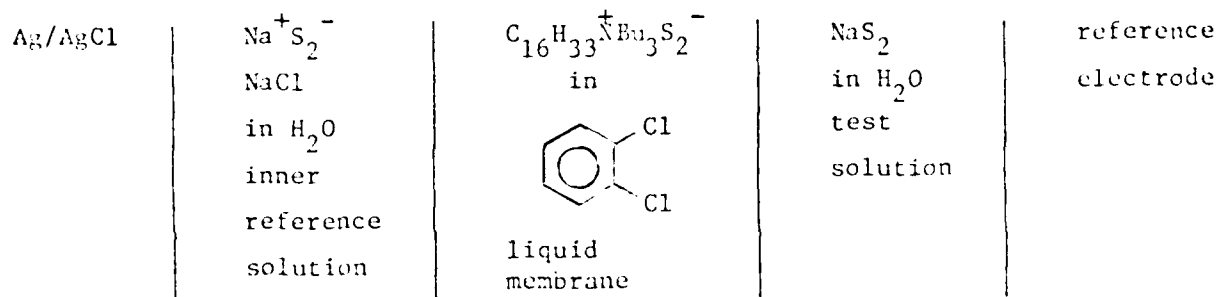


Figure 5. Electrode construction for sensing anionic surfactants.

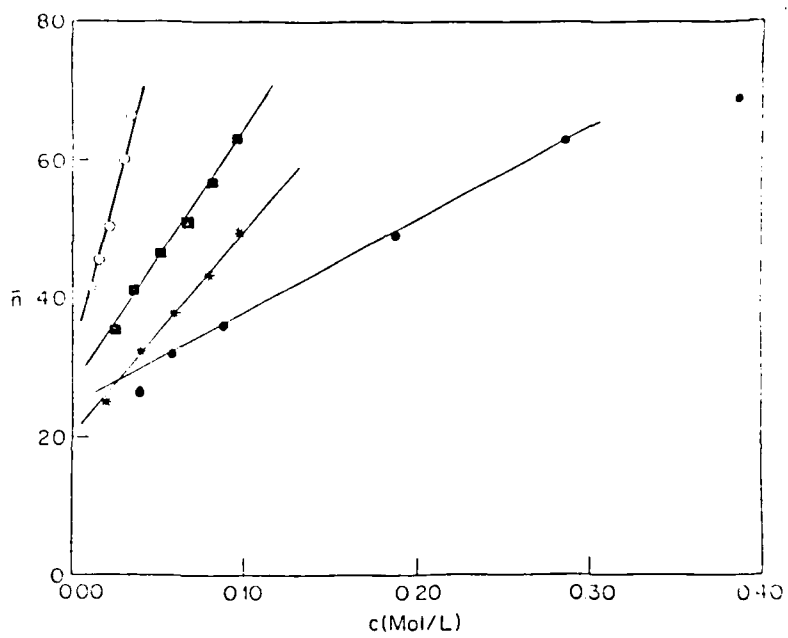


Figure 6. Micellar aggregation number vs. concentration of micellized surfactant: $\bar{n} = 3$ (o); $\bar{n} = 8$ (■); $\bar{n} = 2$ (*); $\bar{n} = 1$ (●).

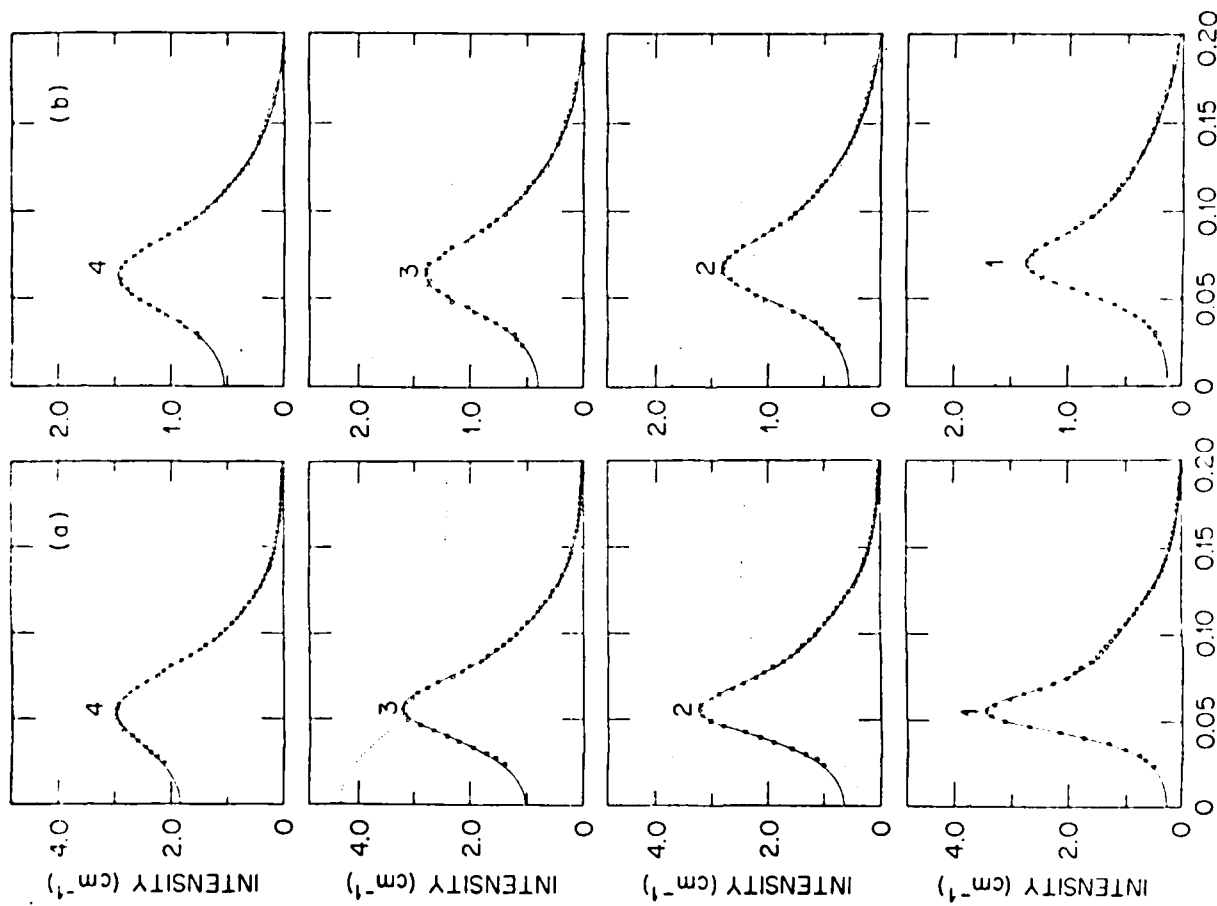


Figure 7. Fit of experimental SANS data as a function of added NaCl for \bar{z} (a) and \bar{g} (b). Full lines: Calculated intensities; dotted line, $S(Q)$; dashed line, $P(Q)$.

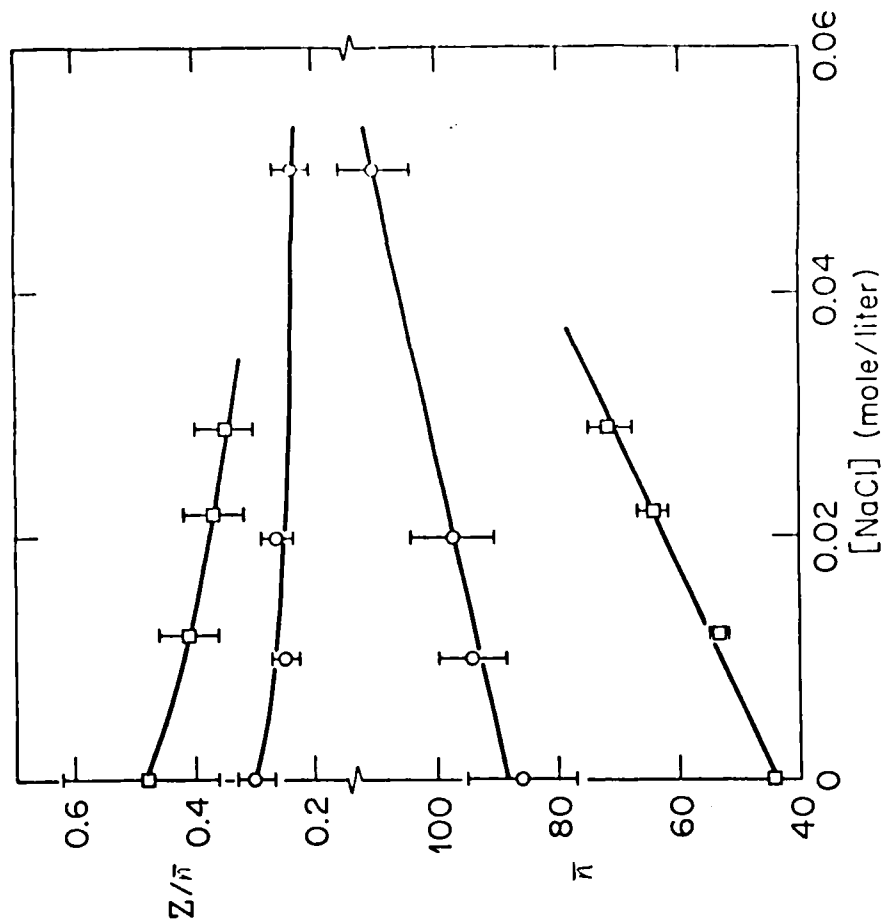


Figure 8. Plot of the aggregation numbers and extent of counterion dissociation for \bar{z} (○) and $\bar{\pi}$ (□)

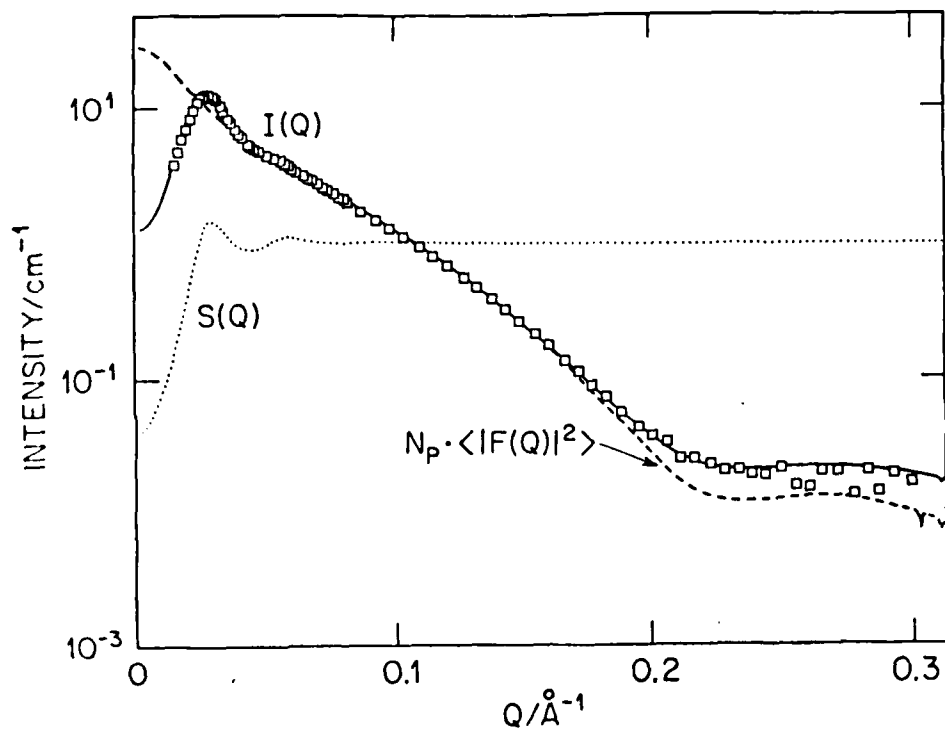


Figure 9. Fit of the scattering curve for 0.041 M $\underline{5}$, assuming the micelles to be prolate ellipsoids.

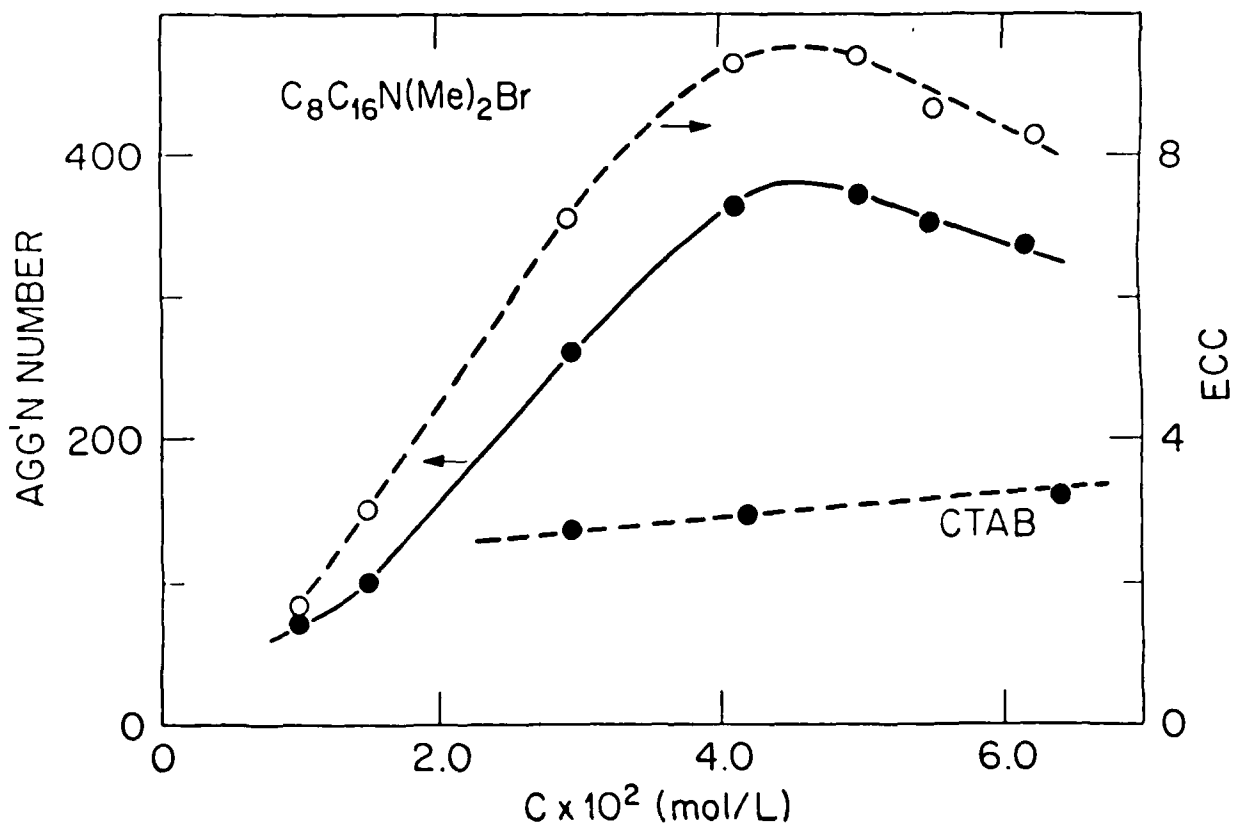
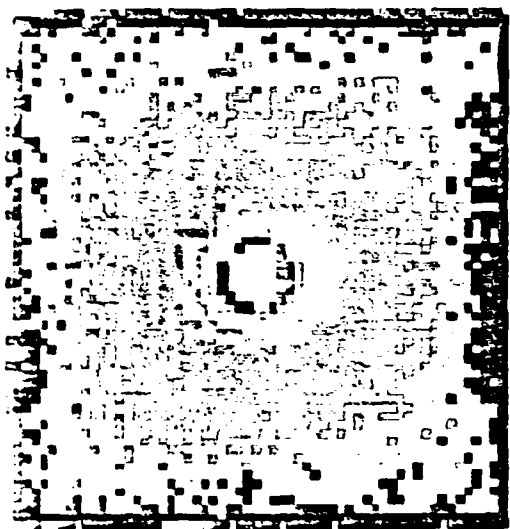
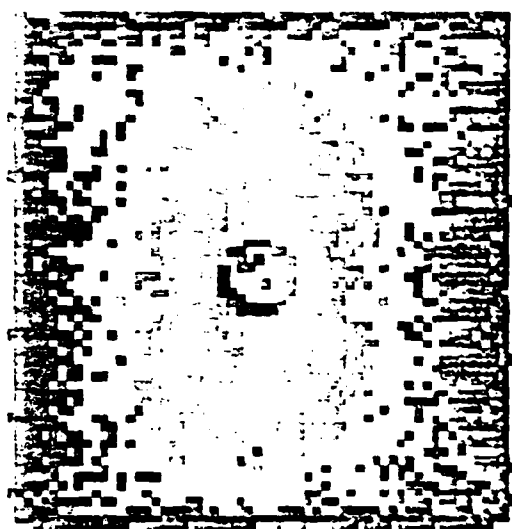


Figure 10. Micellar aggregation numbers for CTAB and $\underline{5}$; axial ratios for $\underline{5}$.

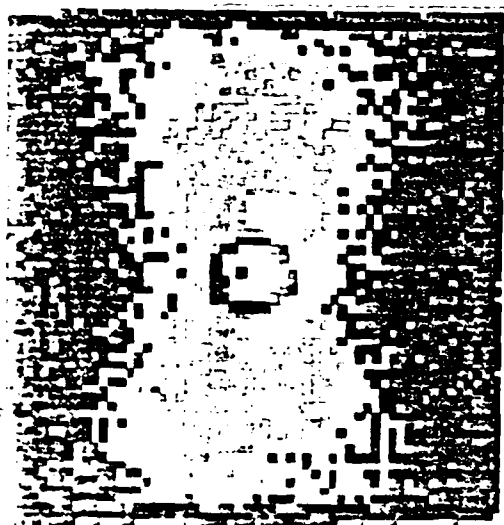
0.01 M $C_8C_{16}N(CH_3)_2Br$ in 0.02 M NaCl at 45°C



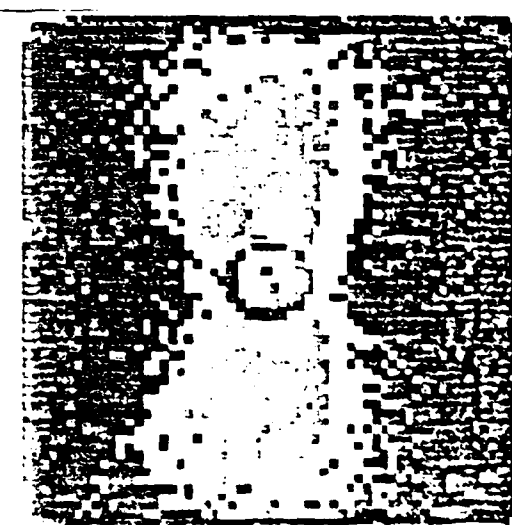
$G = 0 \text{ s}^{-1}$



$G = 810$



$G = 2024$



$G = 2632$

Figure 11. 2-D contour plots of scattered intensities for shear-aligned micellar solutions. G is the shear rate.

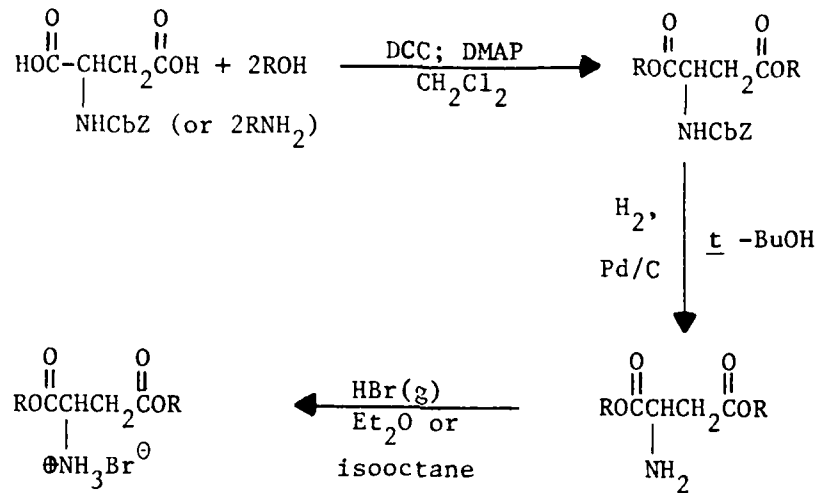
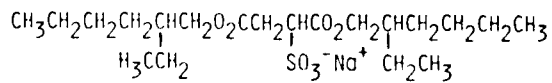


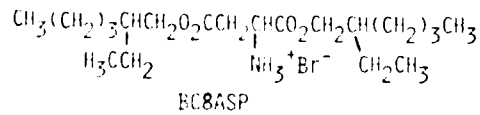
Figure 12: Synthetic scheme for oil-soluble surfactants.

Figure 13

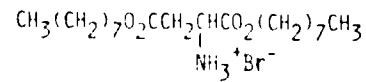
OIL-SOLUBLE SURFACTANTS



Aerosol OT



BC8ASP



NC8ASP

EN